Bone 120 (2019) 327–335

Contents lists available at ScienceDirect

Bone

journal homepage: www.elsevier.com/locate/bone

Full Length Article

SHP2 regulates intramembranous ossification by modifying the TGFβ and BMP2 signaling pathway

Lijun Wang[a], Jiahui Huang[a], Douglas C. Moore[a], Yueming Song[b], Michael G. Ehrlich[a,1], Wentian Yang[a,*]

[a] Department of Orthopaedics, Brown University Alpert Medical School and Rhode Island Hospital, Providence, RI 02903, United States of America
[b] Department of Orthopedic Surgery, West China Hospital of Sichuan University, Chengdu 610041, P.R. China

ARTICLE INFO

Keywords:
SHP2
Intramembranous ossification
Mesenchymal progenitors
Osteoblast differentiation
TGFβ and BMP2 signaling

ABSTRACT

SHP2 is a ubiquitously expressed protein tyrosine phosphatase, which is involved in many signaling pathways to regulate the skeletal development. In endochondral ossification, SHP2 is known to modify the osteogenic fate of osteochondroprogenitors and to impair the osteoblastic transdifferentiation of hypertrophic chondrocytes. However, how SHP2 regulates osteoblast differentiation in intramembranous ossification remains incompletely understood. To address this question, we generated a mouse model to ablate SHP2 in the Prrx1-expressing mesenchymal progenitors by using "Cre-loxP"-mediated gene excision and examined the development of calvarial bone, in which the main process of bone formation is intramembranous ossification. Phenotypic characterization showed that SHP2 mutants have severe defects in calvarial bone formation. Cell lineage tracing and in situ hybridization data showed less osteoblast differentiation of mesenchymal cells and reduced osteogenic genes expression, respectively. Further mechanistic studies revealed enhanced TGFβ and suppressed BMP2 signaling in SHP2 ablated mesenchymal progenitors and their derivatives. Our study uncovered the critical role of SHP2 in osteoblast differentiation through intramembranous ossification and might provide a potential target to treat craniofacial skeleton disorders.

1. Introduction

The skull vault of mammals, providing essential protection for the brain and important sensory organs, consists of the frontal, parietal, inter-parietal and occipital bones, which all undergo intramembranous ossification [1,2]. During development, cell lineage analysis showed that the frontal bones are mainly contributed from the neural crest cells, while parietal and inter-parietal bones originate from the paraxial mesoderm [3–5]. These cells migrate into defined locations overlying the cerebral hemispheres, and subsequently differentiate into osteogenic mesenchyme, which is characterized by the expression of Runt-related transcription factor 2 (RUNX2) and OSTERIX, the earliest molecular determinants of bone formation [6–9]. In contrast to the endochondral ossification that ensues from a cartilaginous anlagen, intramembranous ossification features a direct differentiation of mesenchymal progenitors into osteoblasts, responsible for the synthesis of collagen type 1(COL1α1)-rich bone extracellular matrix and its mineralization.

Protein tyrosine phosphatase non-receptor type 11(*PTPN11*), also known as SHP2, is a widely expressed SH2 domain-containing non-receptor protein tyrosine phosphatase. Accumulating evidences suggest a crucial role of SHP2 in regulation of skeletal development and homeostasis. SHP2 gain-of-function (GOF) mutations cause Noonan Syndrome (NS), which has calvarial abnormality including macrocephaly, oral malformation and hypertelorism [10–12]. Conversely, SHP2 loss-of-function(LOF) mutation cause benign cartilage tumor, metachondromatosis, both in human and in mice [13,14]. Recently, we reported that SHP2 determines the cell fate of osteochondroprogenitors [15] and its specific deletion in collagen type 2(COL2a1) or collagen type 10(COL10a1) expressing chondrocytes impairs the osteoblast transdifferentiation of hypertrophic chondrocyte in endochondral ossification, which indicate SHP2 plays a crucial role in osteoblast differentiation [16]. SHP2 ablation in mesenchymal progenitors cause defects of calvarial bone formation [17], but the cellular and molecular mechanism of how SHP2 regulates osteoblast differentiation and bone formation in calvarial development is not fully understood.

Calvarial development is a complex process consisting both endochondral ossification and intramembranous ossification. Here, we

* Corresponding author at: 1 Hoppin Street, Coro West 402E, Providence, RI 02903, United States of America.
E-mail address: wyang@lifespan.org (W. Yang).
[1] Deceased.

https://doi.org/10.1016/j.bone.2018.11.014
Received 4 September 2018; Received in revised form 7 November 2018; Accepted 20 November 2018
Available online 22 November 2018
8756-3282/

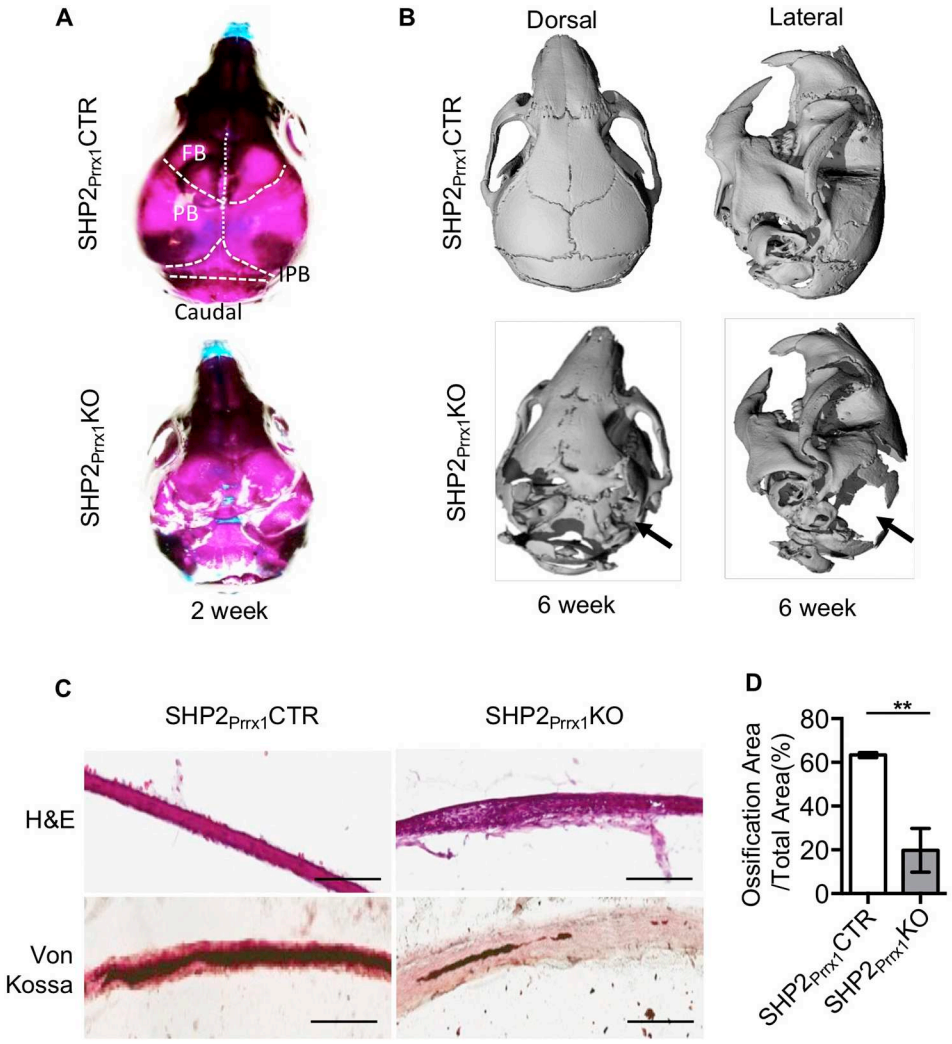

Fig. 1. SHP2 ablation in the *Prrx1*+ mesenchymal cells impairs intramembranous ossification. A. Representative skull images of 2-week-old $SHP2_{Prrx1}CTR$ and $SHP2_{Prrx1}KO$ mice stained with Alcian blue and Alizarin Red. n = 3. B. μ-CT radiographs demonstrating the skull structure of 6-week-old $SHP2_{Prrx1}CTR$ and $SHP2_{Prrx1}KO$ mice. Note that parietal and interparietal bone ossification was defective (arrows) in the $SHP2_{Prrx1}KO$ mice, compared with age matched $SHP2_{Prrx1}CTR$ mice. n = 3. C. Representative H&E (top) and von Kossa (bottom, counterstained by fast red) staining of murine parietal bone coronal frozen sections showing the appearance of a loose mesenchyme tissue and impaired mineralization of the parietal bone in the P0.5 $SHP2_{Prrx1}KO$ mice, compared with $SHP2_{Prrx1}CTR$ mice. Scale bar:100 μm. D. Bar graph showing the quantitative data of parietal bone matrix mineralization in $SHP2_{Prrx1}CTR$ and $SHP2_{Prrx1}KO$ mice using NIH ImageJ software (n = 3, $^{**}p < 0.01$, Student's *t*-test). (For interpretation of the references to colour in this figure legend, the reader is referred to the web version of this article.)

specifically delete SHP2 in mesenchymal progenitors through Prrx1-Cre to investigate the role of SHP2 in the development of parietal and inter-parietal bone, which undergo intramembranous ossification. During the early phases of the parietal and inter-parietal bone formation, mesenchymal progenitors first undergo proliferation and differentiation, leading to the formation of several bony anlagen margined by the osteogenic fronts and connected by the fibrous connective tissue sutures, which are rich in mesenchymal progenitors and fibroblasts. After acquiring the basic shape, each of the skull bony elements remains separated by sutures to ensures that calvarial expansion is coordinated with growth of the underlying brain. Synchronized with the osteoblast-mediated bone formation, calvarial bones also undergo dynamic modeling and remodeling through the coordinated resorptive activity of osteoclasts. These developmental processes at last establish the three-dimensional architecture of the skull.

Lines of genetic and molecular evidence suggest multiple signaling pathways and transcription factors as important regulators of skull development, such as the signaling pathways evoked by BMP/TGFβ [18], FGFs [19], WNT [20] and hedgehog [21] et al. Among these signaling pathways, transforming growth factor beta (TGFβ) and bone morphogenic protein2 (BMP2) are considered as two of the most important signaling pathways to regulate osteogenesis [18,22], both of which are of the TGFβ superfamily. TGFβ ligand binds to TGFβ receptor complex (TGFβR I & TGFβR II) and then phosphorylate SMAD2/3. Similarly, BMP2 ligand binds to BMP receptor complex (BMPR I & BMPR II) and then phosphorylate SMAD1/5/8 [23,24]. TGFβ signaling was demonstrated to promote proliferation and early differentiation of osteoprogenitor, however, it inhibits the maturation, mineralization and transit of osteoblast to osteocyte [18]. In addition, TGFβ treatment blocks osteoblast mineralization in vitro [25]. In contrast, BMP2 signaling has been proved to promote osteogenic differentiation of mesenchymal progenitors and bone formation [22,24]. Furthermore, both TGFβ signaling and BMP2 signaling are reported to regulate osteoblast differentiation by modifying the activity of RUNX2 and OSTERIX [18,26–28], the key osteogenic transcription factors regulating the expression of osteogenic gene programs [29].

In this study, we research on the role of SHP2 in intramembranous ossification of calvarial development at cellular and molecular level. And we demonstrate that SHP2 is critical for osteogenic differentiation of mesenchymal progenitors partially via modifying TGFβ/BMP2 signaling.

2. Materials and methods

2.1. Animals

Tg(*Ptpn11*$^{fl/+}$) [30], *Tg*(*Rosa26*^{ZsG}) [31], *Tg*(*Prrx1-Cre*) [32] and *Tg*(*Sp7-mCherry*) (*Sp7*^{mCherry}) [33] mice were described previously. PCR genotyping methods for the *Ptpn11* floxed allele, *Rosa26*^{ZsG} and *Sp7*^{mCherry} reporters, and Cre transgene are reported in the original publications and are available upon request. Mice bearing *Ptpn11* floxed alleles were bred to *Tg*(*Prrx1-Cre*) mice to generate offspring in which SHP2 was deleted in osteochondroprogenitors (OCPs) that express the paired related homeobox-1 protein PRRX1, and controls. The mice had

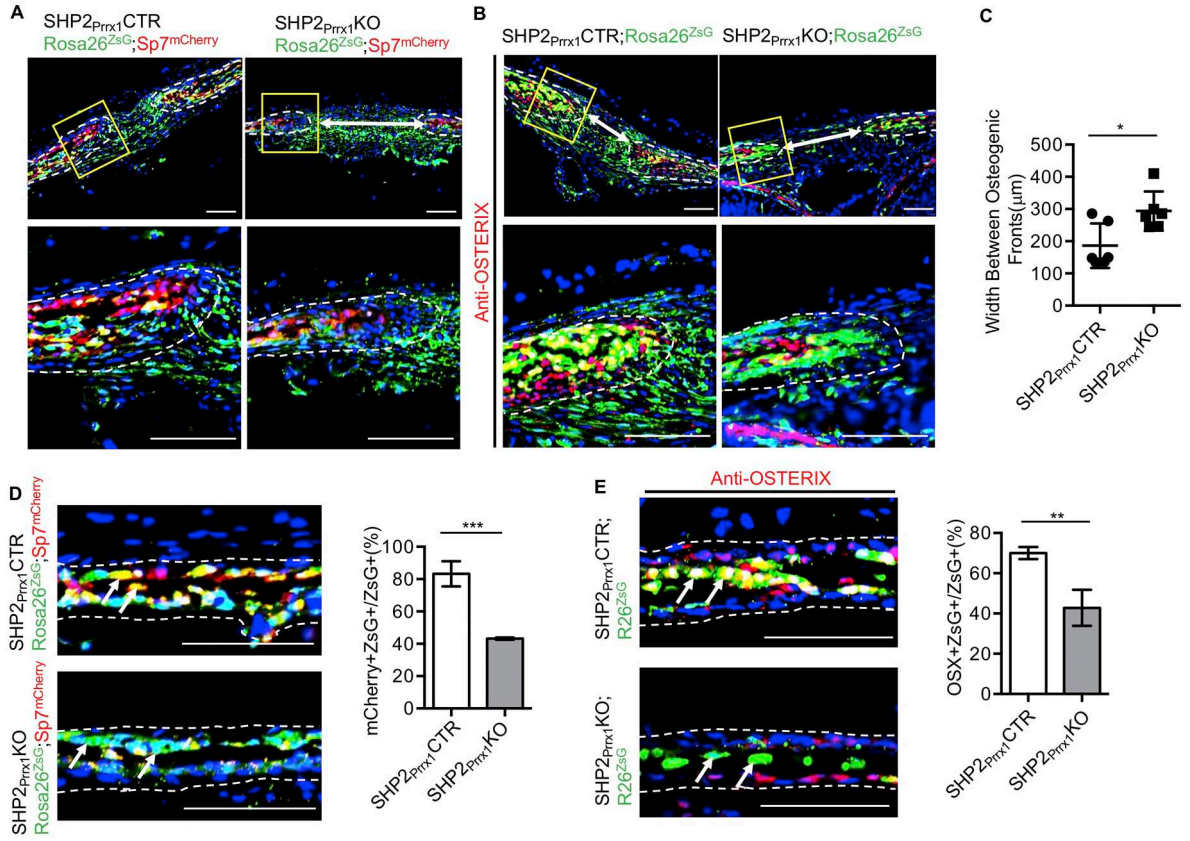

Fig. 2. SHP2 is required for the osteogenic differentiation of the *Prrx1* + mesenchymal cells. A. Fluorescent images of the sagittal sutures showing the number and location of *Prrx1* + (green), *Osx* + (red), and *Prrx1/Osx* double positive cells (yellow) at the osteogenic fronts and sutures. Note that the number of *Prrx1 and Osx* double positive cells decreased and the width of the sagittal suture (white arrows) increased significantly in $SHP2_{Prrx1}KO;Rosa26^{ZsG};Sp7^{mCherry}$ mice, compared with the $SHP2_{Prrx1}CTR;Rosa26^{ZsG};Sp7^{mCherry}$ controls. Images at the bottom are the enlarged views of the corresponding boxed areas in the top images. Scale bar: 100 μm. B. Sagittal sutures of indicated mice immunostained with anti-OSTERIX antibody (red) showing the number and location of *Prrx1* + (green), OSTERIX + (red), and *Prrx1*/OSTERIX double positive cells (yellow) at the osteogenic fronts and sutures. Images at the bottom are the enlarged views of the corresponding boxed areas in the top images. Scale bar: 100 μm. Scale bar: 100 μm. C. Bar graphs showing the quantitative data of sagittal suture width (images of A and B) in the P0.5 $SHP2_{Prrx1}CTR$ and the $SHP2_{Prrx1}KO$ mice (n = 6, $*p < 0.05$, Student's *t*-test). D-E. Fluorescent images of the parietal bone frozen sections showing the number and location of *Prrx1* + (green), Osx + (red), OSTERIX + (red), and *Prrx1 and Osx* (OSTERIX) double positive (yellow) cells in the indicated mice. Quantitative data are shown as bar graphs on the right (n = 3, $***p < 0.001$, Student's *t*-test) Scale bar: 100 μm. (For interpretation of the references to colour in this figure legend, the reader is referred to the web version of this article.)

the following genotypes and nomenclature: $Tg(Prrx1\text{-}Cre;Ptpn11^{fl/+})$ ($SHP2_{Prrx1}CTR$) and $Tg(Prrx1\text{-}Cre;Ptpn11^{fl/fl})$ ($SHP2_{Prrx1}KO$). $SHP2_{Prrx1}CTR$ and $SHP2_{Prrx1}KO$ mice were also bred with $Rosa26^{ZsG}$ and $Sp7^{mCherry}$ reporter mice for experiments designed to trace the fate of *Prrx1*-expressing cells in vivo. All of the mice were maintained on the C57BL/6 J background.

Control and SHP2 mutant animals were sacrificed at the indicated time points and explanted skull tissue was processed for micro-computed tomographic imaging (μCT), histological sectioning, and biochemical and biological analyses. All animal work was reviewed and approved by the Rhode Island Hospital Institutional Animal Care and Use Committee and performed in accordance with PHS policy on the humane care and use of laboratory animals.

2.2. Osteoblast isolation and cultures

Primary osteoblastic cells were isolated from calvarias of the $SHP2_{Prrx1}CTR;Rosa26^{ZSG}$ and $SHP2_{Prrx1}KO;Rosa26^{ZSG}$ newborns. To do so, the parietal bones were collected under sterile condition and digested with 5 ml of Trypsin-EDTA (0.06%), and Collagenase II (285 U/ml) for 4 h. The digestion was halted by adding an equal volume of DMEM with 10% FBS, and the digestion solution was passed through a 40 μm strainer to obtain single cells. Osteoblasts were collected by centrifugation and resuspended in fresh culture medium (DMEM with 10% FBS,1% penicillin and streptomycin). Osteoblast cell preparations were cultured at 37° C under 5% CO_2.

Primary osteoblasts were immortalized with retrovirus expressing pBabe(puro)/SV40 large T antigen prepared from 293 T cells, as described previously [16], [30,34]. Infected cells were cultured for 48 h and then selected with puromycin for 7 days, after which the puromycin-resistant clones were pooled and expanded. Finally, the osteoblastic cells were enriched by FACS sorting based on the $Rosa26^{ZsG}$ GFP fluorophore.

2.3. Reagents

Polyclonal antibodies against murine SHP2 (sc-280) and SMAD1 (sc-7965) were purchased from Santa Cruz Biotechnology, and monoclonal anti-Sp7/OSTERIX (ab22552) was purchased from Abcam. Monoclonal antibodies against murine phospho-SMAD2/3 (8828S) and total SMAD2/3 (3102S) were purchased from Cell Signaling Technology, p-SMAD1/5/8 (AB3848) was purchased from Millipore, and anti-β-ACTIN (ab8226) was purchased from Abcam. Texas Red-X goat anti-rabbit IgG (T6391) was purchased from Invitrogen. 1% Alcian blue and 1% Alizarin Red staining solutions were purchased from Poly Scientific. Click-iT EdU Alexa Fluor 594 Imaging Kit(C10339) was purchased from Life Technology.

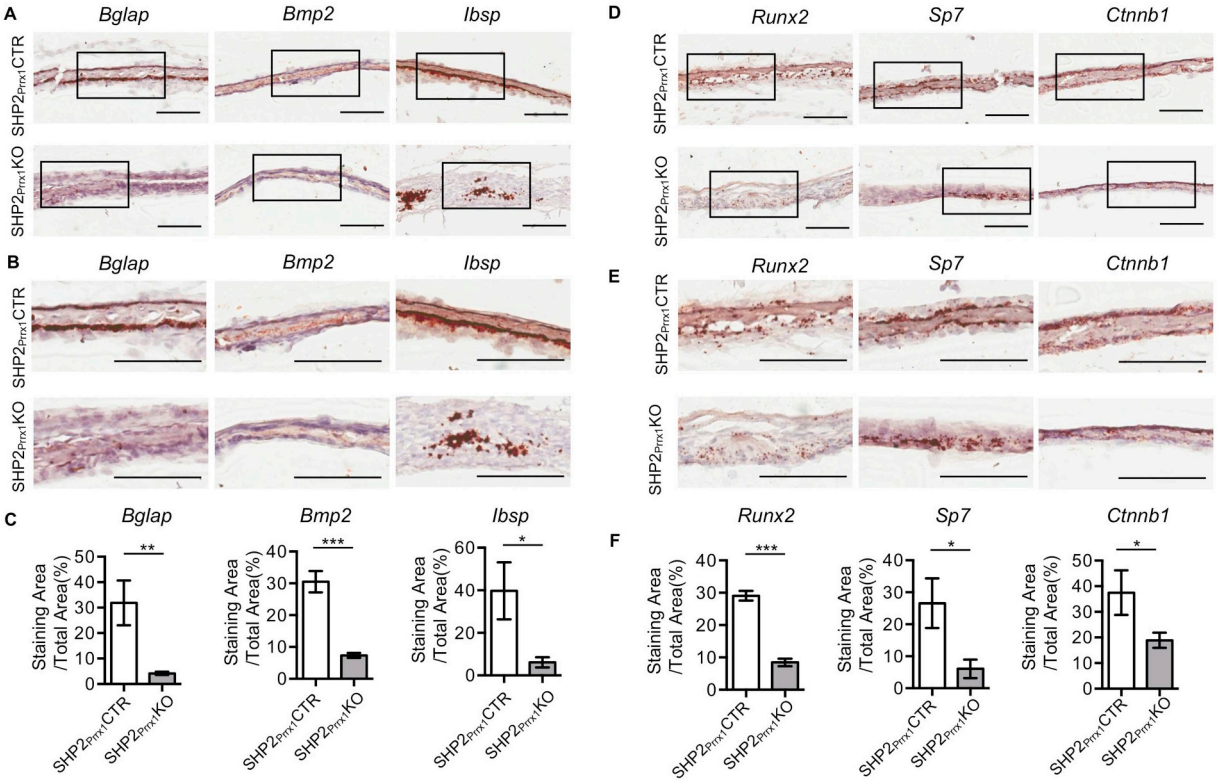

Fig. 3. SHP2 deletion in the *Prrx1*-expressing mesenchymal cells impairs osteogenic marker genes and osteogenic transcription factors expression during intramembranous ossification. A. RNAscope-based in situ hybridization showing the transcript abundance of indicated osteogenic genes in the P0.5 parietal bone of $SHP2_{Prrx1}$CTR and $SHP2_{Prrx1}$KO mice. Scale bar: 100 μm. B. Enlarged views of the corresponding boxed areas in A. Scale bar: 100 μm. C. Bar graphs showing the quantitative data of A & B. Data presented as the ratio of the positive staining areas vs. the corresponding total areas using NIH ImageJ (n = 3, $*p < 0.05$, $**p < 0.01$, $***p < 0.001$, Student's *t*-test). D. The transcript abundance of indicated osteogenic transcription factors in the P0.5 parietal bone of $SHP2_{Prrx1}$CTR and $SHP2_{Prrx1}$KO mice were presented as described in A. Scale bar: 100 μm. E. Enlarged views of the corresponding boxed areas in D. Scale bar: 100 μm. F. Bar graphs showing the quantitative data of D & E. Data presented as the ratio of the positive staining areas vs. the corresponding total areas using NIH ImageJ (n = 3, $*p < 0.05$, $**p < 0.01$, $***p < 0.001$, Student's t-test).

2.4. Histological, histochemical and immunostaining analysis

Skulls from P0.5 control and SHP2 mutants were fixed in 4% formaldehyde, soaked in 30% sucrose solution for 24 h, and embedded in OCT. Frozen sections were stained with hematoxylin and eosin (H&E) and von Kossa (Millipore) to visualize general morphology and bone matrix mineralization, respectively. The fate of *Prrx1*-expressing mesenchymal cells in vivo was determined by direct visualization of the ZsGreen+ (green), mCherry+ (red), and ZsGreen/mCherry double positive (yellow) fluorophores on frozen sections of parietal bone from $SHP2_{Prrx1}$CTR;$Rosa26^{ZsG}$;$Sp7^{mCherry}$ and $SHP2_{Prrx1}$KO;$Rosa26^{ZsG}$;$Sp7^{mCherry}$ mice. DAPI was used for nucleus counterstaining. All florescent and phase contrast images were captured using a Nikon digital fluorescence microscope and Aperio slide scanner (Leica Biosystems).

For Immunofluorescent staining, frozen sections were blocked with 0.3%Triton X-100, and 10% goat serum in PBS for 2 h at room temperature, after which they were incubated with primary antibody overnight (1:100 dilution). After washing, the primary antibodies were localized with Texas Red-X goat anti-rabbit IgG secondary antibody. Nuclei were counter- stained with DAPI.

2.5. In situ hybridization

mRNA expression was determined using RNAscope in situ hybridization, as described previously [16]. Probes against murine *Runx2*, *Sp7*, *Ctnnb1*, *Bmp2*, *Ibsp,* and *Bglap* were synthesized and purchased through Advanced Cell Diagnostics (ACD). Visualization of the hybridized probes was achieved using the RNAscope® HD-Brown kit (Advanced Cell Diagnostics). Images of each section were acquired using the Aperio slide scanner.

Osteogenic gene expression was quantified on corresponding 200 μm × 100 μm areas in the same regions of the parietal bones from $SHP2_{Prrx1}$CTR and $SHP2_{Prrx1}$KO mice. The positively-stained area and the total bone tissue area were quantified using NIH ImageJ software.

2.6. Quantitative RT-PCR and micro-CT analyses

Total RNA was extracted from cultured osteoblasts using the RNeasy kit (Qiagen). cDNA was synthesized using 1 μg of total RNA with iScript™cDNA Synthesis Kit (Bio-Rad) and qRT-PCR was performed with RT^2SYBR®Green kit on a Bio-Rad CFX machine. All samples were normalized to *Gapdh* and *Actin*, and gene expression was presented as fold increases or decreases compared with that of control. High resolution (20 μm isometric voxel size) 3D volume images were generated using a desktop μ-CT40 system (Scanco Medical AG, CH).

2.7. Western blot analysis

Cells were lysed in modified NP-40 lysis buffer (0.5% NP40, 150 mM NaCl, 1 mM EDTA, 50 mM Tris [pH 7.4]) supplemented with a protease inhibitor cocktail (1 mM PMSF, 10 mg/ml aprotinin, 0.5 mg/ml antipain, and 0.5 mg/ml pepstatin) [35]. Cell lysates (20–30 μg) were separated by SDS-PAGE, transferred to PVDF membranes, and incubated with indicated primary antibodies for 2 h or overnight at 4 °C (primary antibody concentration is 1 μg/ml); this was followed by HRP-conjugated secondary antibodies (Bio-Rad, 1:2000 dilution).

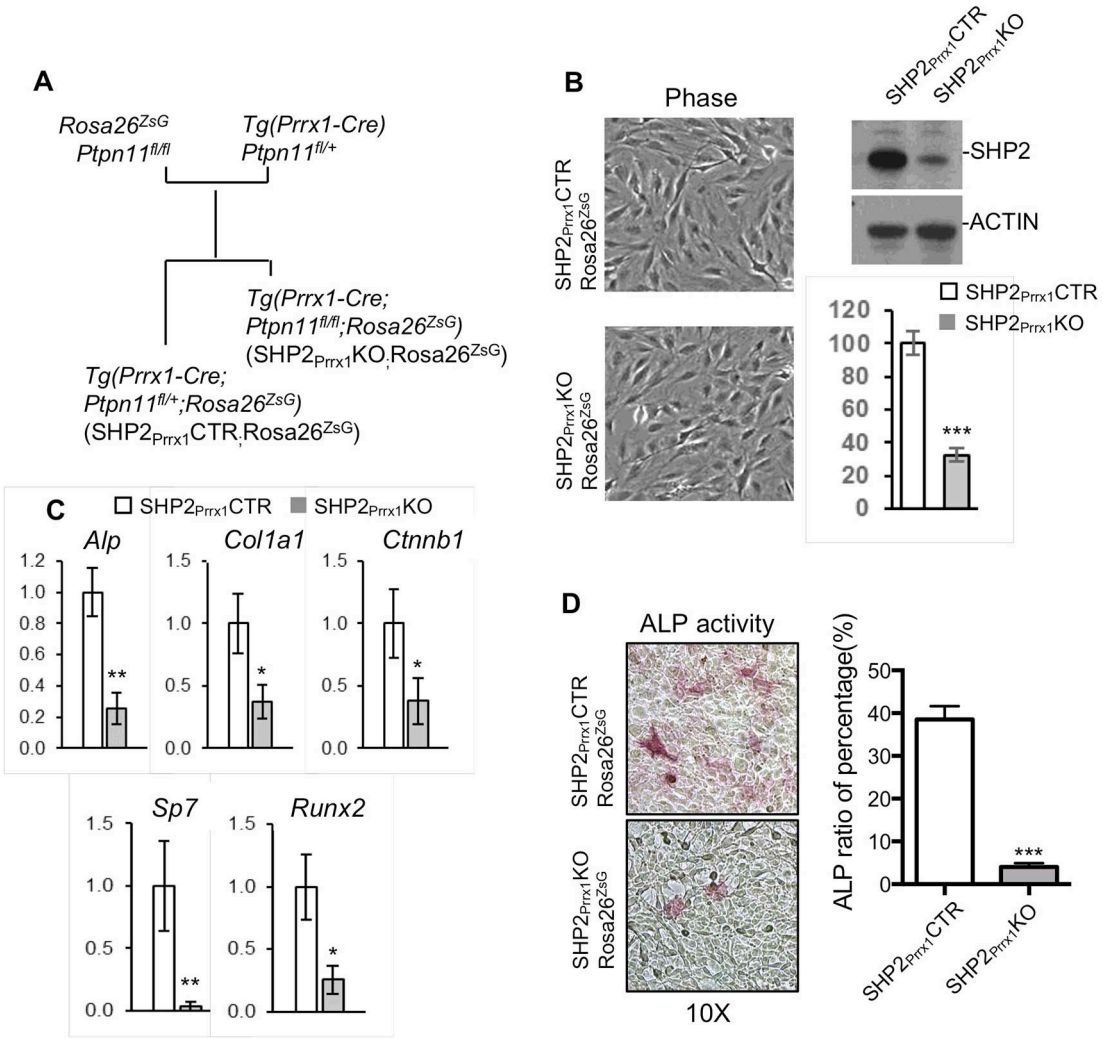

Fig. 4. SHP2 deletion in the *Prrx1*-expressing cells compromises osteogenic genes expression in vitro. A. Diagram denotes the strategy to generate SV40 large T antigen-immortalized osteoblasts from the $SHP2_{Prrx1}CTR;Rosa26^{ZsG}$ and $SHP2_{Prrx1}KO;Rosa26^{ZsG}$ mice. B. Phase contrast images (left) showing the morphology of immortalized osteoblasts. Western blot and bar graphs [44] demonstrating the level of SHP2 in the immortalized osteoblasts from indicated mice (n = 3, $^{***}p < 0.001$, Student's t-test). C. Bar graphs showing the relative expression of indicated osteogenic genes in $SHP2_{Prrx1}CTR$ and $SHP2_{Prrx1}KO$ osteoblasts determined by qRT-PCR. (n = 3, $^{*}p < 0.05$, $^{**}p < 0.01$, Student's t-test). D. Phase contrast images demonstrating ALP activity in the immortalized osteoblastic cells from indicated mice. Ratio of ALP positive cells vs total cells in the defined areas are presented as bar graphs on the right (n = 3, $^{***}p < 0.001$, Student's t-test).

2.8. Statistical analysis

Differences between the SHP2 knockouts and controls were evaluated using Student's *t*-tests, with p values < 0.05 considered to be significant. Statistical analyses were performed by using Prism 5.0 (GraphPad, San Diego, CA) and Excel (Microsoft).

3. Results

3.1. SHP2 deletion in the Prrx1-expressing mesenchymal cells impairs calvarial bone ossification

$SHP2_{Prrx1}KO$ mutants were born at the expected Mendelian ratios, but they were smaller than their control littermates [15]. Most of the SHP2 mutants died within 3 weeks after birth, likely due to difficulty with breathing and feeding, but a few of the mutant mice could survive until 6 weeks [15]. Compared with the $SHP2_{Prrx1}CTR$ mice, the skulls of $SHP2_{Prrx1}KO$ mice were incompletely formed. Alcian blue and Alizarin Red staining revealed marked defects in mineralization of the parietal, interparietal, and occipital bones (Fig. 1A), as well as the tibiae, femur and humerus, which are of endochondral origin [15]. These findings were even more striking in the data from the μCT imaging, where the parietal and interparietal bones were totally absent in the models created from the thresholded μCT images of 6-week-old $SHP2_{Prrx1}KO$ mice (Fig. 1B, bottom), while the skulls of the $SHP2_{Prrx1}CTR$ mice appear entirely normal, with intact cranial vaults and well-defined sutures (Fig. 1B, top).

Histological analysis of stained frozen sections was performed to evaluate the microarchitecture of the skull elements. H&E and von Kossa staining of the sections from P0.5 $SHP2_{Prrx1}CTR$ mice revealed a sandwich-like morphology in which the fully mineralized parietal bone was covered by two layers of soft periosteal mesenchymal tissue (Fig. 1C left). In contrast, mineralization of the parietal bone was markedly reduced in P0.5 $SHP2_{Prrx1}KO$ mutants as the von Kossa staining image showed (Fig. 1C right). Instead, there was a dense layer of soft connective tissue filled with undifferentiated mesenchymal cells where the parietal bone should have been. Quantitative analysis revealed a ~70% reduction in the portion of the parietal "bone" tissue that was mineralized in the $SHP2_{Prrx1}KO$ mice compared to corresponding regions of $SHP2_{Prrx1}CTR$ mice (19.8 ± 5.7% vs 63.3 ± 0.6%, $^{**}p < 0.01$) (Fig. 1D). And finally, calcified osteogenic fronts appeared clearly in the $SHP2_{Prrx1}CTR$ mice but were absent in the

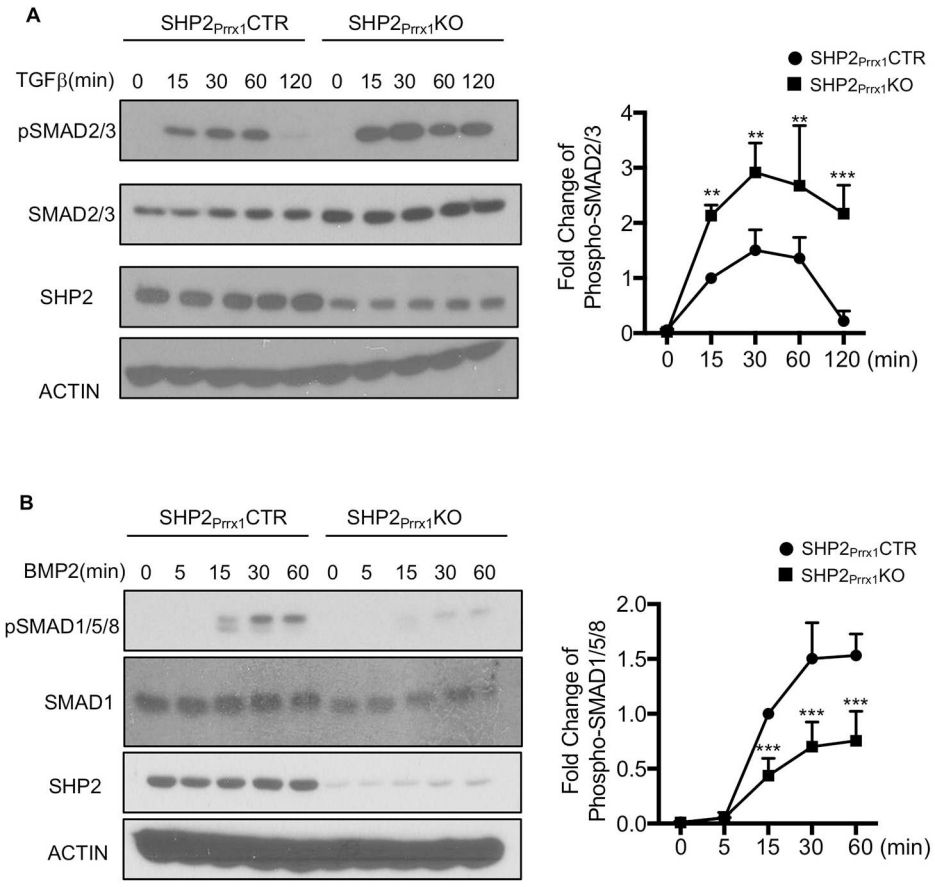

Fig. 5. SHP2 differentially regulates TGFβ and BMP signaling pathways. A. Immunoblotting data show that TGFβ-evoked SMAD2/3 phosphorylation was enhanced in the osteoblastic cells from $SHP2_{Prrx1}KO$ mice, compared to that from $SHP2_{Prrx1}CTR$ mice. Cells were starved overnight and stimulated with TGFβ (100 ng/ml) for indicated time points. Phosphorylation of SMAD2/3 was quantified using NIH ImageJ software and normalized to the β-ACTIN controls, the phosphorylation level of SMAD2/3 was corrected by the total level of SMAD2/3. (n = 3, $^{**}p < 0.01$, $^{***}p < 0.001$, Student's t-test) B. Immunoblotting data showing decreased SMAD1/5/8 phosphorylation in response to BMP2 in $SHP2_{Prrx1}KO$ osteoblastic cells, compared to $SHP2_{Prrx1}CTR$ osteoblastic cells. Cells were starved overnight and stimulated with BMP2 (100 ng/ml) for indicated time points. Phosphorylation of SMAD1/5/8 was quantified as described in A (n = 3, $^{**}p < 0.01$, $^{***}p < 0.001$, Student's t-test).

$SHP2_{Prrx1}KO$ mice (Fig. S1). Taken together, these data indicate that SHP2 expression in the *Prrx1*-expressing OCPs is essential for the mineralization of calvarial bones.

3.2. SHP2 is required for the osteogenic differentiation of the Prrx1 + mesenchymal progenitors

Having established that lack of SHP2 in *Prrx1*-expressing OCPs inhibits intramembranous ossification, we next sought to determine whether the cause might be lack of OCP differentiation. To start, we performed a dual fluorescent reporter-based cell lineage tracing study. $SHP2_{Prrx1}CTR;Rosa26^{ZsG}$ and $SHP2_{Prrx1}KO;Rosa26^{ZsG}$ mice were bred with $Sp7^{mCherry}$ reporter mice, with the idea that the resulting $SHP2_{Prrx1}CTR;Rosa26^{ZsG};Sp7^{mCherry}$ and $SHP2_{Prrx1}KO;Rosa26^{ZsG};Sp7^{mCherry}$ mice would express ZsGreen in cells that expressed, or had expressed, *Prrx1* + (i.e. osteochondral progenitors and their progeny), and mCherry in cells that expressed *Sp7* (i.e. osteoblast lineage cells). Importantly, if the *Prrx1* + ZsGreen cells differentiated into *Sp7*-expressing osteoblastic cells, they would co-express the ZsGreen and mCherry reporters, which would appear yellow. As shown in Fig. 2A (left) & D(top), a large number of cells within the osteogenic fronts and the parietal bones fluoresced yellow in the $SHP2_{Prrx1}CTR;Rosa26^{ZsG};Sp7^{mCherry}$ mice. The yellow cells at the osteogenic fronts were connected by soft tissue bridge rich in ZsGreen + cells, which indicated they were *Prrx1* + mesenchymal progenitors. In contrast, the number of yellow cells in the osteogenic fronts and in the parietal bone were significantly reduced in the $SHP2_{Prrx1}KO;Rosa26^{ZsG};Sp7^{mCherry}$ mutants (43.19 ± 0.37% vs. 83.24 ± 4.48%, $^{***}p < 0.001$, Student's *t*-test) (Fig. 2A & D). Instead, a large quantity of green cells was observed in the $SHP2_{Prrx1}KO;Rosa26^{ZsG};Sp7^{mCherry}$ mutants. This suggests that the maturation of *Prrx1* + green cells into osteoblasts was compromised in the absence of SHP2. The above observations were bolstered by immunostaining of the parietal bone frozen sections with the Texas-red labeled anti-OSTERIX antibodies ($SHP2_{Prrx1}CTR;Rosa26^{ZsG}$ vs. $SHP2_{Prrx1}KO;Rosa26^{ZsG}$: mean ± SEM of percentage: 70.02 ± 1.75 vs. 42.84 ± 5.17, $^{**}p < 0.01$, Student's *t*-test) (Fig. 2B & E). Consistent with these observations, the width of sagittal suture significantly increased in the SHP2 mutants, compared to the controls (186.2 ± 28.1 μm vs. 293.9 ± 24.9 μm, $^{*}p < 0.05$, Student's t-test) (Fig. 2C). Taken together, these data suggest that lack of SHP2 in OCPs inhibits their osteogenic differentiation during intramembranous ossification.

3.3. SHP2 deletion in the Prrx1-expressing mesenchymal progenitors suppresses osteogenic gene expression

Calvarial bones ossify through intramembranous ossification in which mesenchymal progenitors undergo progressive differentiation into osteoblasts, which express OSTERIX (*Sp7*), COL1a1, bone sialoprotein, and OSTEOCALCIN. RUNX2 has been considered the master gene of osteoblast differentiation [6,8]. RUNX2 is considered essential for the osteogenic differentiation of the *Prrx1* + mesenchymal progenitors but it is not required for the terminal differentiation of the *Col1a1* + osteoblasts [36]. Having demonstrated that SHP2 is indispensable for the differentiation of OCPs into functioning osteoblasts, we next explored whether the expression of *Runx2* and other osteogenic genes were affected in these mutants. RNAScope®-based in situ hybridization revealed significant reductions in *Runx2*, *Sp7*, *Ctnnb1*, *Bglap*, *Bmp2* and *Ibsp* transcripts in frozen sections of parietal bone from the $SHP2_{Prrx1}KO$ mutants, compared with the $SHP2_{Prrx1}CTR$ controls (Fig. 3). These data are consistent with the von Kossa staining data showing an impaired mineralization of the parietal bones (Fig. 1C). Collectively, these data indicate that SHP2 regulates the osteogenic differentiation of OCPs in intramembranous ossification by modulating

the expression of the osteogenic transcription factors, as well as downstream effecting osteoblastic genes.

3.4. SHP2 is required for osteogenic gene expression in the Prrx1+ progenitors and their derivatives

We used cell culture to gain additional insight into the molecular and cellular mechanisms through which SHP2 regulates intramembranous ossification. To do so we isolated ZsGreen+ calvarial cells from the $SHP2_{Prrx1}CTR;Rosa26^{ZsG}$ and $SHP2_{Prrx1}KO;R26^{ZsG}$ mice via FACS and immortalized them via the retroviral expression of SV40 large T antigen (Fig. 4A). Phase contrast images showed that immortalized calvarial cells from both control and SHP2 mutant mice display bipolar or multipolar and elongated shapes, and western blotting confirmed that the SHP2 protein level was significantly reduced in the osteoblastic cells from the $SHP2_{Prrx1}KO;Rosa26^{ZsG}$ mice, compared with $SHP2_{Prrx1}CTR;Rosa26^{ZsG}$ control animals (only about 30% of the controls) (Fig. 4B). qRT-PCR revealed significant reductions in the transcript abundance of osteogenic genes *Alp*, *Col1a1*, *Ctnnb1*, *Sp7* and *Runx2* in the $SHP2_{Prrx1}KO;Rosa26^{ZsG}$ cells, compared to the $SHP2_{Prrx1}CTR;Rosa26^{ZsG}$ controls (Fig. 4C). ALP activity was also evaluated in the $SHP2_{Prrx1}KO;Rosa26^{ZsG}$ cells and $SHP2_{Prrx1}CTR;Rosa26^{ZsG}$ controls using a colorimetric assay. The number of positively-stained cells and total cells were counted in three fields of view and analyzed. The quantitative data showed that the ALP activity was markedly reduced in the SHP2 mutant cells (mean ± SEM of percentage: 38.53 ± 1.80 vs. 4.00 ± 0.53, $^{***}p < 0.001$, Student's *t*-test) (Fig. 4D). These data in vitro confirmed our in vivo findings that SHP2 is required for intramembranous ossification by promoting the osteogenic gene expression.

3.5. SHP2 regulates osteogenic gene expression by modifying the TGFβ and BMP2 signaling pathways

TGFβ and BMP2 signaling has a fundamental role in the regulation of embryonic skeletal development and maintaining postnatal bone homeostasis via the regulation of RUNX2 and osteogenic gene expression [18]. Because our data indicated that impaired osteogenic differentiation of SHP2-deficient OCPs involved reductions in *Runx2* and other osteogenic genes, we sought to investigate whether SHP2 might influence the TGFβ/BMP2 signaling axis. To do so, calvarial osteoblast cell lines from $SHP2_{Prrx1}CTR$ and $SHP2_{Prrx1}KO$ mice were starved overnight and then harvested at 0, 15, 30, 60 and 120 min after stimulation with TGFβ (100 ng/ml). Western blotting revealed that the SMAD2/3 phosphorylation was significantly increased in $SHP2_{Prrx1}KO$ cells compared to the $SHP2_{Prrx1}CTR$ control cells (Fig. 5A). Moreover, the phosphorylation level of SMAD2/3 returned to basal levels 120mins after stimulation in the $SHP2_{Prrx1}CTR$ cells but remained high in $SHP2_{Prrx1}KO$ cells (Fig. 5A). We also starved $SHP2_{Prrx1}CTR$ and $SHP2_{Prrx1}KO$ cells overnight, stimulated them with BMP2 (100 ng/ml) and then harvested at 0, 5, 15, 30 and 60 min. The western blot data revealed that the phosphorylation level of SMAD1/5/8 was significantly decreased in $SHP2_{Prrx1}KO$ cells, compared to $SHP2_{Prrx1}CTR$ control cells under the same stimulation (Fig. 5B). These data indicate that SHP2 normally represses the phosphorylation of SMAD2/3 by TGFβR I but promotes the phosphorylation of SMAD1/5/8 by BMPR I; these coupled but differential regulation of TGFβ and BMP2 signaling pathway to ensure the maturation and function of osteoblasts.

4. Discussion

Intramembranous ossification is regulated by a number of signaling pathways, in which protein tyrosine kinases are heavily involved [18,19]. Increasing evidences suggest that protein tyrosine phosphatases play a crucial role in this process, too. SHP2 is a ubiquitously expressed PTP. Early studies showed that SHP2 is a key modulator of the osteogenic differentiation of OCPs [15] and growth plate hypertrophic chondrocytes by modifying SOX9 abundance during endochondral ossification [16]. Here, we showed that SHP2 is indispensable for the osteogenic differentiation of OCPs in the calvarial bones. SHP2 deficient OCPs were halted at the primitive stages and failed to ossify the matrix of the forming calvarial vault (Figs. 1 & 2), rather than a defect in cell proliferation (Fig. S3). Consistent with these morphological defects, transcript abundance of osteogenic transcription factors *Runx2* and *Osterix* and their downstream effectors (Figs. 3 & 4) were found significantly decreased in the SHP2 mutants. Importantly, SHP2 was uncovered to differentially regulate canonical BMP2 (promoting) and TGFβ (suppressing) signaling in OCPs and their derivatives in vitro (Fig. 5). Collectively, our study uncovered an important role for SHP2 in intramembranous ossification by modulating the osteogenic differentiation and maturation of OCPs, these actions, in part, are via the differential regulation of BMP and TGFβ signaling pathways.

BMP and TGFβ signaling pathways are well accepted as one of the most important signaling pathways to regulate osteoblast differentiation and maturation. TGFβ signaling pathway promotes osteoblastic progenitor proliferation and early differentiation but suppresses the osteoblastic maturation, mineralization, and transit to osteocyte [18]. Upon TGFβ signaling pathway activation, SMAD2/3 is phosphorylated and then recruit class II deacetylases (HDACs 4 and 5) to repress the gene expression and activity of *Runx2* [37–40]. In contrast, activation of the BMP signaling pathway regulates osteoblast differentiation. Activated BMPR I phosphorylates SMAD1/5/8, which up-regulates the expression of *Runx2* and *Osterix* and drive osteoblastic differentiation [37–39]. Our immunoblotting data showed that SHP2 deficiency in osteoblast promoted TGFβ-evoked SMAD2/3 phosphorylation and suppressed BMP2-evoked SMAD1/5/8 activation (Fig. 5), indicating that SHP2 differentially regulates the BMP and TGFβ signaling pathways and osteoblast differentiation and maturation. This could explain why there was a wider gap between the osteogenic fronts in the sagittal suture of SHP2 mutants and accumulation of primitive Prrx1+ osteochondroprogenitors. *Runx2* and *Osterix* are considered as the two master transcription factors during osteoblastogenesis [26–28]. The profound resemblance of the skull phenotype between SHP2 and RUNX2 mutants suggests that RUNX2 functions downstream SHP2 [36]. This notion was further supported by the reduction of RUNX2 responsive osteogenic gene expression (Fig. 4) in SHP2 mutants [18,27,41,42].

TGFβ and BMP2 also signal via SMAD independent non-canonical pathways, in which, they activate TAK1 and TAK1-binding protein1(TAB1) to initiate the MKKs and ERK signaling cascade [22]. TGFβ and BMP2 evoked MKK activation could positively regulate *Runx2* expression and promote the differentiation of OCPs [43]. We, therefore, examined TGFβ and BMP2-evoked ERK activation in osteoblasts and found that they were comparable in the presence or absence of SHP2 (Fig. S2), suggesting that SHP2 regulation of BMP and TGFβ signaling primarily went through the canonical TGFβ/SMAD2/3 and BMP2/SMAD1/5/8 signaling pathways.

BMP and TGFβ signal through BMPR I/II and TGFR I/II respectively to phosphorylate SMAD1/5/8 and SMAD2/3 and activate their downstream transcription programs [44]. Altered SMAD phosphorylation in SHP2 deficient OCPs and their derivatives suggest that SHP2 acts either on a serine/threonine kinase upstream of SMADs or SMAD phosphatases. SHP2 functions a PTP, therefore the effect of SHP2 on BMP2- and TGFβ-evoked SMAD phosphorylation must be mediated via an indirect mechanism. Currently, we are investigating whether TGFβ and BMP2 receptor kinase activity is modulated by phosphorylation of tyrosine residues [45].

In sum, SHP2 is found to be essential for the osteogenic

differentiation and maturation of OCPs and intramembranous ossification, partially by differentially modifying the TGFβ and BMP signaling pathways. SHP2 and its signaling partner(s) could potentially serve as pharmacological targets to treat craniofacial disorders, such as craniosynostosis and cleidocranial dysostosis.

Acknowledgements

This publication was made possible by NIH and the National Institute for General Medicine Sciences (NIGMS) Grant #8P20GM103468 and NIAMS RO1AR066746 (WY). This work was also in part supported by the Rhode Island Hospital Orthopaedic Foundation and Arthritis National Research Foundation (WY). LW is a pilot award recipient from NIGMS1P20 GM119943.

Author contributions

LW, JH, DCM, and WY contributed to data collection; DCM conducted μCT data collection and analysis; YS and MGE contributed important intellectual content; LW, DCM, and WY wrote the manuscript. All authors read and approve the final version of this manuscript.

Disclosures

All authors state that they have no conflicts of interest.

Appendix A. Supplementary data

Supplementary data to this article can be found online at https://doi.org/10.1016/j.bone.2018.11.014.

References

[1] S.W. Jin, K.B. Sim, S.D. Kim, Development and growth of the Normal cranial vault : an embryologic review, J. Korean Neurosurg. Soc. 59 (3) (2016) 192–196.
[2] M. Ishii, J. Sun, M.C. Ting, R.E. Maxson, The development of the calvarial bones and sutures and the pathophysiology of craniosynostosis, Curr. Top. Dev. Biol. 115 (2015) 131–156.
[3] X. Jiang, S. Iseki, R.E. Maxson, H.M. Sucov, G.M. Morriss-Kay, Tissue origins and interactions in the mammalian skull vault, Dev. Biol. 241 (1) (2002) 106–116.
[4] T. Yoshida, P. Vivatbutsiri, G. Morriss-Kay, Y. Saga, S. Iseki, Cell lineage in mammalian craniofacial mesenchyme, Mech. Dev. 125 (9–10) (2008) 797–808.
[5] R.A. Deckelbaum, G. Holmes, Z. Zhao, C. Tong, C. Basilico, C.A. Loomis, Regulation of cranial morphogenesis and cell fate at the neural crest-mesoderm boundary by engrailed 1, Development 139 (7) (2012) 1346–1358.
[6] P. Ducy, R. Zhang, V. Geoffroy, A.L. Ridall, G. Karsenty, Osf2/Cbfa1: a transcriptional activator of osteoblast differentiation, Cell 89 (5) (1997) 747–754.
[7] T. Koga, Y. Matsui, M. Asagiri, T. Kodama, B. de Crombrugghe, K. Nakashima, H. Takayanagi, NFAT and Osterix cooperatively regulate bone formation, Nat. Med. 11 (8) (2005) 880–885.
[8] T. Komori, H. Yagi, S. Nomura, A. Yamaguchi, K. Sasaki, K. Deguchi, Y. Shimizu, R.T. Bronson, Y.H. Gao, M. Inada, M. Sato, R. Okamoto, Y. Kitamura, S. Yoshiki, T. Kishimoto, Targeted disruption of Cbfa1 results in a complete lack of bone formation owing to maturational arrest of osteoblasts, Cell 89 (5) (1997) 755–764.
[9] K. Nakashima, X. Zhou, G. Kunkel, Z. Zhang, J.M. Deng, R.R. Behringer, B. de Crombrugghe, The novel zinc finger-containing transcription factor osterix is required for osteoblast differentiation and bone formation, Cell 108 (1) (2002) 17–29.
[10] T. Araki, M.G. Mohi, F.A. Ismat, R.T. Bronson, I.R. Williams, J.L. Kutok, W. Yang, L.I. Pao, D.G. Gilliland, J.A. Epstein, B.G. Neel, Mouse model of Noonan syndrome reveals cell type- and gene dosage-dependent effects of Ptpn11 mutation, Nat. Med. 10 (8) (2004) 849–857.
[11] M. Tartaglia, E.L. Mehler, R. Goldberg, G. Zampino, H.G. Brunner, H. Kremer, I. van der Burgt, A.H. Crosby, A. Ion, S. Jeffery, K. Kalidas, M.A. Patton, R.S. Kucherlapati, B.D. Gelb, Mutations in PTPN11, encoding the protein tyrosine phosphatase SHP-2, cause Noonan syndrome, Nat. Genet. 29 (4) (2001) 465–468.
[12] K. Kosaki, T. Suzuki, K. Muroya, T. Hasegawa, S. Sato, N. Matsuo, R. Kosaki, T. Nagai, Y. Hasegawa, T. Ogata, PTPN11 (protein-tyrosine phosphatase, non-receptor-type 11) mutations in seven Japanese patients with Noonan syndrome, J. Clin. Endocrinol. Metab. 87 (8) (2002) 3529–3533.
[13] M.E. Bowen, E.D. Boyden, I.A. Holm, B. Campos-Xavier, L. Bonafe, A. Superti-Furga, S. Ikegawa, V. Cormier-Daire, J.V. Bovee, T.C. Pansuriya, S.B. de Sousa, R. Savarirayan, E. Andreucci, M. Vikkula, L. Garavelli, C. Pottinger, T. Ogino, A. Sakai, B.M. Regazzoni, W. Wuyts, L. Sangiorgi, E. Pedrini, M. Zhu, H.P. Kozakewich, J.R. Kasser, J.G. Seidman, K.C. Kurek, M.L. Warman, Loss-of-function mutations in PTPN11 cause metachondromatosis, but not Ollier disease or Maffucci syndrome, PLoS Genet. 7 (4) (2011) e1002050.
[14] H.K. Kim, O. Aruwajoye, D. Sucato, B.S. Richards, G.S. Feng, D. Chen, P.D. King, N. Kamiya, Induction of SHP2 deficiency in chondrocytes causes severe scoliosis and kyphosis in mice, Spine (Phila Pa 1976) 38 (21) (2013) E1307–E1312.
[15] C. Zuo, L. Wang, R.M. Kamalesh, M.E. Bowen, D.C. Moore, M.S. Dooner, A.M. Reginato, Q. Wu, C. Schorl, Y. Song, M.L. Warman, B.G. Neel, M.G. Ehrlich, W. Yang, SHP2 regulates skeletal cell fate by modifying SOX9 expression and transcriptional activity, Bone Res. 6 (2018) 12.
[16] L. Wang, J. Huang, D.C. Moore, C. Zuo, Q. Wu, L. Xie, K. von der Mark, X. Yuan, D. Chen, M.L. Warman, M.G. Ehrlich, W. Yang, SHP2 regulates the osteogenic fate of growth plate hypertrophic chondrocytes, Sci. Rep. 7 (1) (2017) 12699.
[17] P.E. Lapinski, M.F. Meyer, G.S. Feng, N. Kamiya, P.D. King, Deletion of SHP-2 in mesenchymal stem cells causes growth retardation, limb and chest deformity, and calvarial defects in mice, Dis. Model. Mech. 6 (6) (2013) 1448–1458.
[18] M. Wu, G. Chen, Y.P. Li, TGF-beta and BMP signaling in osteoblast, skeletal development, and bone formation, homeostasis and disease, Bone Res. 4 (2016) 16009.
[19] D.M. Ornitz, P.J. Marie, FGF signaling pathways in endochondral and intramembranous bone development and human genetic disease, Genes Dev. 16 (12) (2002) 1446–1465.
[20] J.B. Regard, Z. Zhong, B.O. Williams, Y. Yang, Wnt signaling in bone development and disease: making stronger bone with Wnts, Cold Spring Harb. Perspect. Biol. 4 (12) (2012).
[21] T.F. Day, Y. Yang, Wnt and hedgehog signaling pathways in bone development, J. Bone Joint Surg. Am. 90 (Suppl. 1) (2008) 19–24.
[22] G. Chen, C. Deng, Y.P. Li, TGF-beta and BMP signaling in osteoblast differentiation and bone formation, Int. J. Biol. Sci. 8 (2) (2012) 272–288.
[23] M.J. Goumans, C. Mummery, Functional analysis of the TGFbeta receptor/Smad pathway through gene ablation in mice, Int. J. Dev. Biol. 44 (3) (2000) 253–265.
[24] X. Cao, D. Chen, The BMP signaling and in vivo bone formation, Gene 357 (1) (2005) 1–8.
[25] T. Matsunobu, K. Torigoe, M. Ishikawa, S. de Vega, A.B. Kulkarni, Y. Iwamoto, Y. Yamada, Critical roles of the TGF-beta type I receptor ALK5 in perichondrial formation and function, cartilage integrity, and osteoblast differentiation during growth plate development, Dev. Biol. 332 (2) (2009) 325–338.
[26] K.S. Lee, H.J. Kim, Q.L. Li, X.Z. Chi, C. Ueta, T. Komori, J.M. Wozney, E.G. Kim, J.Y. Choi, H.M. Ryoo, S.C. Bae, Runx2 is a common target of transforming growth factor beta1 and bone morphogenetic protein 2, and cooperation between Runx2 and Smad5 induces osteoblast-specific gene expression in the pluripotent mesenchymal precursor cell line C2C12, Mol. Cell. Biol. 20 (23) (2000) 8783–8792.
[27] M.H. Lee, T.G. Kwon, H.S. Park, J.M. Wozney, H.M. Ryoo, BMP-2-induced Osterix expression is mediated by Dlx5 but is independent of Runx2, Biochem. Biophys. Res. Commun. 309 (3) (2003) 689–694.
[28] H. Kurata, P.V. Guillot, J. Chan, N.M. Fisk, Osterix induces osteogenic gene expression but not differentiation in primary human fetal mesenchymal stem cells, Tissue Eng. 13 (7) (2007) 1513–1523.
[29] K. Nakashima, B. de Crombrugghe, Transcriptional mechanisms in osteoblast differentiation and bone formation, Trends Genet. 19 (8) (2003) 458–466.
[30] W. Yang, J. Wang, D.C. Moore, H. Liang, M. Dooner, Q. Wu, R. Terek, Q. Chen, M.G. Ehrlich, P.J. Quesenberry, B.G. Neel, Ptpn11 deletion in a novel progenitor causes metachondromatosis by inducing hedgehog signalling, Nature 499 (7459) (2013) 491–495.
[31] L. Madisen, T.A. Zwingman, S.M. Sunkin, S.W. Oh, H.A. Zariwala, H. Gu, L.L. Ng, R.D. Palmiter, M.J. Hawrylycz, A.R. Jones, E.S. Lein, H. Zeng, A robust and high-throughput Cre reporting and characterization system for the whole mouse brain, Nat. Neurosci. 13 (1) (2010) 133–140.
[32] M. Logan, J.F. Martin, A. Nagy, C. Lobe, E.N. Olson, C.J. Tabin, Expression of Cre Recombinase in the developing mouse limb bud driven by a Prxl enhancer, Genesis 33 (2) (2002) 77–80.
[33] S. Strecker, Y. Fu, Y. Liu, P. Maye, Generation and characterization of Osterix-Cherry reporter mice, Genesis 51 (4) (2013) 246–258.
[34] W.C. Hahn, S.K. Dessain, M.W. Brooks, J.E. King, B. Elenbaas, D.M. Sabatini, J.A. DeCaprio, R.A. Weinberg, Enumeration of the simian virus 40 early region elements necessary for human cell transformation, Mol. Cell. Biol. 22 (7) (2002) 2111–2123.
[35] W. Yang, L.D. Klaman, B. Chen, T. Araki, H. Harada, S.M. Thomas, E.L. George, B.G. Neel, An Shp2/SFK/Ras/Erk signaling pathway controls trophoblast stem cell survival, Dev. Cell 10 (3) (2006) 317–327.
[36] T. Takarada, R. Nakazato, A. Tsuchikane, K. Fujikawa, T. Iezaki, Y. Yoneda, E. Hinoi, Genetic analysis of Runx2 function during intramembranous ossification, Development 143 (2) (2016) 211–218.
[37] J. Li, K. Tsuji, T. Komori, K. Miyazono, J.L. Wrana, Y. Ito, A. Nifuji, M. Noda, Smad2 overexpression enhances Smad4 gene expression and suppresses CBFA1 gene expression in osteoblastic osteosarcoma ROS17/2.8 cells and primary rat calvaria cells, J. Biol. Chem. 273 (47) (1998) 31009–31015.
[38] T. Alliston, L. Choy, P. Ducy, G. Karsenty, R. Derynck, TGF-beta-induced repression of CBFA1 by Smad3 decreases cbfa1 and osteocalcin expression and inhibits osteoblast differentiation, EMBO J. 20 (9) (2001) 2254–2272.
[39] A.B. Hjelmeland, S.H. Schilling, X. Guo, D. Quarles, X.F. Wang, Loss of Smad3-mediated negative regulation of Runx2 activity leads to an alteration in cell fate determination, Mol. Cell. Biol. 25 (21) (2005) 9460–9468.

[40] J.S. Kang, T. Alliston, R. Delston, R. Derynck, Repression of Runx2 function by TGF-beta through recruitment of class II histone deacetylases by Smad3, EMBO J. 24 (14) (2005) 2543–2555.
[41] A.B. Celil, J.O. Hollinger, P.G. Campbell, Osx transcriptional regulation is mediated by additional pathways to BMP2/Smad signaling, J. Cell. Biochem. 95 (3) (2005) 518–528.
[42] M.H. Lee, Y.J. Kim, H.J. Kim, H.D. Park, A.R. Kang, H.M. Kyung, J.H. Sung, J.M. Wozney, H.J. Kim, H.M. Ryoo, BMP-2-induced Runx2 expression is mediated by Dlx5, and TGF-beta 1 opposes the BMP-2-induced osteoblast differentiation by suppression of Dlx5 expression, J. Biol. Chem. 278 (36) (2003) 34387–34394.
[43] C.F. Lai, S.L. Cheng, Signal transductions induced by bone morphogenetic protein-2 and transforming growth factor-beta in normal human osteoblastic cells, J. Biol. Chem. 277 (18) (2002) 15514–15522.
[44] K.H. Wrighton, X. Lin, X.H. Feng, Phospho-control of TGF-beta superfamily signaling, Cell Res. 19 (1) (2009) 8–20.
[45] C.H. Heldin, K. Miyazono, P. ten Dijke, TGF-beta signalling from cell membrane to nucleus through SMAD proteins, Nature 390 (6659) (1997) 465–471.